Oxidized Multiwalled Carbon Nanotubes as Effective Reinforcement and Thermal Stability Agents of Poly(lactic acid) Ligaments

ARTICLE *in* JOURNAL OF APPLIED POLYMER SCIENCE · DECEMBER 2010

Impact Factor: 1.77 · DOI: 10.1002/app.32626

Oxidized Multiwalled Carbon Nanotubes as Effective Reinforcement and Thermal Stability Agents of Poly(lactic acid) Ligaments

K. Chrissafis,[1] K. M. Paraskevopoulos,[1] A. Jannakoudakis,[2] T. Beslikas,[3] D. Bikiaris[4]

[1]*Solid State Physics Department, School of Physics, Aristotle University of Thessaloniki, GR-541 24, Thessaloniki, Macedonia, Greece*
[2]*Laboratory of Physical Chemistry, Department of Chemistry, Aristotle University of Thessaloniki, GR-541 24, Thessaloniki, Macedonia, Greece*
[3]*2nd Orthopedic Department, Aristotle University of Thessaloniki, Macedonia, Greece*
[4]*Laboratory of Polymer Chemistry and Technology, Department of Chemistry, Aristotle University of Thessaloniki, GR-541 24, Thessaloniki, Macedonia, Greece*

Received 5 January 2010; accepted 13 April 2010
DOI 10.1002/app.32626
Published online 29 June 2010 in Wiley InterScience (www.interscience.wiley.com).

ABSTRACT: In this study, nanocomposites of poly(lactic acid) (PLA) containing 0.5, 1, and 2.5 wt % oxidized multiwalled carbon nanotubes (MWCNT–COOHs) were prepared by the solved evaporation method. From transmission electron microscopy and scanning electron microscopy micrographs, we observed that the MWCNT–COOHs were well dispersed in the PLA matrix and, additionally, there was increased adhesion between PLA and the nanotubes. As a result, all of the studied nanocomposites exhibited higher mechanical properties than neat PLA; this indicated that the MWCNT–COOHs acted as efficient reinforcing agents, whereas in the nonoxidized multiwalled carbon nanotubes, the mechanical properties were reduced. Nanotubes can act as nucleating agents and, thereby, affect the thermal properties of PLA and, especially, the crystallization rate, which is faster than that of neat PLA. From the thermogravimetric data, we observed that the PLA/MWCNT–COOH nanocomposites presented relatively better thermostability than PLA; this was also verified from the calculation of activation energy. On the contrary, the addition of MWCNT–COOH had a negative effect on the enzymatic hydrolysis rate of PLA. © 2010 Wiley Periodicals, Inc. J Appl Polym Sci 118: 2712–2721, 2010

Key words: biomaterials; nanocomposites; thermal properties

INTRODUCTION

Biodegradable polymers have attracted increased interest over the past 2 decades in fundamental research and in the chemical industry. With the term *biodegradable* are characterized materials that are hydrolyzable at temperatures up to 50°C (e.g., in composting) over a period of several months to 1 year. As a result of hydrolysis, biodegradable polymers break down in physiological environments by macromolecular chain scission into smaller fragments and, ultimately, into simple stable end products.[1,2]

Among the numerous polyesters studied so far, poly(lactic acid) (PLA) has proven to be the most attractive and useful biodegradable polymer.[3] PLA is a biodegradable, biocompatible, and compostable polyester derived from renewable resources, such as corn, potato, cane molasses, and beet sugar. It is the most promising environmentally friendly thermoplastic.[4] It is widely used in various medical applications for controlled drug delivery, medical implants, and absorbable sutures. The use of synthetic degradable polyesters in surgery as suture materials and bone-fixation devices has 3 decades of history.[5] A large number of investigations have been carried out on PLA and its copolymers in biomedical applications for resorbable medical implants.[6,7] Furthermore, PLA can be used in the forms of rod, plate, screw, fiber, sheet, sponge, and beads for bone and tissue engineering; in the form of microspheres in drug-delivery systems;[8,9] and in the form of films or foils for wound treatment and applications in agriculture, such as mulch films, that present the slow release of pesticides and fertilizers.

PLA-based fracture fixation devices have considerably lower tensile moduli than metallic ones, but they can be improved during fabrication with high-modulus fiber reinforcement. Further improvement can be achieved by the incorporation into the PLA matrix of several nanoparticles, such as SiO_2, montmorillonite, and carbon nanotubes.[10–15] These studies have also focused on the crystallization enhancement

Correspondence to: D. Bikiaris (dbic@chem.auth.gr).

of PLA by the incorporation of nanoparticles. Furthermore, some studies have reported the thermal degradation and thermal stability of PLA.[16] The calculated values of the activation energy (E) present a great dispersion, whereas a first-order kinetic reaction has been used in few studies for the determination of E. Also, there have been few studies proposing that the degradation process is followed by more complex kinetics. Kim et al.[17] studied the thermal degradation of PLA-*graft*-MWCNT, and the values of E calculated with Kissinger's and Ozawa's methods were 143.7 and 150.7 kJ/mol, respectively, for PLA/MWCNT and 151.2 and 160.1 kJ/mol, respectively, for PLA/PLA-*g*-MWCNT.[17]

In this study, commercial PLA resorbable reinforcement ligaments, that is, Resorbaid, which is used for the repair and reinforcement of articular instabilities, were studied. The main purpose of this study was to increase the mechanical and mainly thermal properties of the PLA by the incorporation of oxidized multiwalled carbon nanotubes (MWCNT–COOHs) into the polymer matrix. Carbon nanotubes were chosen because they are biocompatible materials and have a high elastic modulus, approaching 1 TPa, and exceptional tensile strengths, ranging from 20 to 100 GPa. Furthermore, oxidation was used to increase the adhesion of the multiwalled carbon nanotubes (MWCNTs) to the PLA matrix.

EXPERIMENTAL

Materials

Commercial reinforcement ligaments consisted of PLA, under the trade name Resorbaid, and were obtained from Cousin Biotech (Wervicq Sud, France). The MWCNTs used in this study were synthesized by a chemical vapor deposition process and were supplied by Nanothinx (Patra, Greece). Their diameters were between 9 and 20 nm, their lengths were greater than 5 μm, and they were used in an oxidized form (MWCNT–COOH). Samples (1 g) of the nanotubes were suspended in 40 mL of a mixture of concentrated nitric acid and sulfuric acid (1 : 3 volume ratio) and were refluxed for 15 min. After they were washed with deionized water until the supernatant attained a pH of around 7, the samples were dried *in vacuo* at 100°C.[18] Dichloromethane anhydrous (≥99.8%) and tetrahydrofuran anhydrous (≥99.8%) were obtained from Aldrich Chemical Co. (Steinheim, Germany).

Preparation of the PLA/MWCNTs nanocomposites

PLA ligaments were dissolved in a mixture of dichloromethane and tetrahydrofuran 50/50 w/w at room temperature, whereas in the same mixture were dispersed MWCNT–COOHs under sonication for 1 h. The PLA solution and MWCNT–COOH dispersion were mixed under stirring for 1 h and sonicated for an additional 1 h. The mixture was maintained at room temperature for 24 h for solvent evaporation and dried *in vacuo* at 60°C for 24 h. The prepared films were placed in a desiccator to prevent any moisture absorption. With this procedure, nanocomposites containing 0.5, 1, and 2.5 wt % MWCNT–COOHs were prepared. Also, for comparison purposes, an additional sample was prepared containing 2.5 wt % untreated MWCNTs.

Mechanical properties

Measurements of the tensile properties of the prepared nanocomposites were performed on an Instron 3344 dynamometer in accordance with ASTM D 638 at a crosshead speed of 5 mm/min. Thin sheets about 350 ± 25 μm in thickness were prepared with an Otto Weber Type PW 30 hydraulic press (Remshalden, Germany) connected to an Omron E5AX temperature controller (Remshalden, Germany) at a temperature of 190 ± 5°C. The molds were rapidly cooled by immersion in water at 20°C. From these sheets, dumbbell-shaped tensile test specimens (the central portions were 5 × 0.5 mm thick with a 22-mm gauge length) were cut in a Wallace cutting press and conditioned at 25°C and 55–60% relative humidity for 48 h. The values of Young's modulus, yield stress, elongation at break, and tensile strength at the break point (σ_b) were determined. At least five specimens were tested for each sample, and the average values, together with the standard deviations, are reported.

Dynamic mechanical analysis (DMA)

The dynamic thermomechanical properties of the nanocomposites were measured with a Rheometric Scientific analyzer (model Mk III) (Pittsfield, USA). The bending method was used at a frequency of 1 Hz and a strain level of 0.04% in the temperature range of 0–90°C. The heating rate (β) was 3°C/min. Testing was performed with rectangular bars with dimensions of approximately 30 × 10 × 3 mm^3. These were prepared with a hydraulic press, as described previously. The exact dimensions of each sample were measured before the testing.

Scanning electron microscopy (SEM)

SEM was carried out with a JEOL JMS-840A scanning microscope (Tokyo, Japan). For this purpose, fractured surfaces of the PLA/MWCNT–COOH nanocomposites in liquid nitrogen were used. All of the studied surfaces were coated with carbon black to avoid charging under the electron beam.

Transmission electron microscopy (TEM)

Electron diffraction and TEM observations were performed on ultrathin film samples of the various nanocomposites, which were prepared by an ultramicrotome. These thin films were deposited on copper grids. A JEOL 120 CX microscope operating at 120 kV was used.

Differential scanning calorimetry (DSC)

The thermal behavior of the polymers was studied with a PerkinElmer Pyris Diamond differential scanning calorimeter (Waltham, MA). The instrument was calibrated with high-purity indium and zinc standards. Samples of about 5 mg were used and heated from 20 to 200°C with a heating rate (β) of 20°C/min. At that temperature (200°C), the samples were kept for 5 min; they were then were cooled to 20°C at a cooling rate of 300°C/min and heated again to 200°C. From these scans, the melting temperature (T_m), cold crystallization temperature (T_{cc}), and glass-transition temperature (T_g) were determined. The crystallization temperature (T_c) from the melt was also recorded by the cooling of the samples from 200 to 60°C at a cooling rate of 20°C/min.

Thermogravimetric (TG) analysis

TG analysis was carried out with a SETARAM SETSYS TG-DTA 16/18 instrument (Caluire, France). Samples (6.0 ± 0.2 mg) were placed in alumina crucibles. An empty alumina crucible was used as a reference. PLA nanocomposites were heated from ambient temperature to 450°C in a 50 mL/min flow of N_2 at heating rates (β's) of 5, 10, 15, and 20°C/min. During these scans, the sample temperature, sample weight, its first derivative, and the heat flow were recorded.

Enzymatic hydrolysis

PLA and its nanocomposites containing different amounts of MWCNT–COOHs in the form of films 3 × 3 cm^2 in size and approximately 0.2 mm thick, prepared by melt-pressing with a hydraulic press, were placed in Petri dishes containing phosphate buffer solution (pH 7.2) with 0.09 mg/mL *Rhizopus delemar* lipase and 0.01 mg/mL *Pseudomonas cepacia* lipase. The Petri dishes were then incubated at 50 ± 1°C in an oven for several days, and the media were replaced every 3 days. After a specific period of incubation, the films were removed from the Petri dishes, washed with distilled water, and weighed to a constant weight. The degree of enzymatic hydrolysis was estimated from the mass loss.

RESULTS AND DISCUSSION

Mechanical properties of the PLA/MWCNT–COOH nanocomposites

MWCNTs as a reinforcement agent can be effectively used in polymer matrices only when a uniform dispersion is achieved. Inhomogeneities and aggregate formation may lead to structural defects. However, obtaining a uniform dispersion of carbon nanotubes in the polymer matrix is very difficult because of the insolubility of the carbon nanotubes and the inherently poor compatibility between them and the polymers.

In a previous study, to enhance the compatibility between PLA and MWCNTs, acrylic acid grafted PLA and hydroxyl-functionalized multiwalled carbon nanotubes (MWCNT–OHs) were used to replace PLA and MWCNTs, respectively.[15] There was a dramatic enhancement in the thermal and mechanical properties of PLA because of the formation of ester groups through the reaction between the carboxylic acid groups of PLA-*g*-acrylic acid and the hydroxyl groups of MWCNT–OH. The formation of covalent bonds between PLA and MWCNTs that leads to grafting reactions has been used extensively to enhance the adhesion between the two materials.[19–21] MWCNT functionalization can be achieved in a much simpler way by chemical oxidation with a mixture of sulfuric and nitric acids, and this was used in this study. The used time for acid treatment was 15 min because, as was found from our previous study,[18] many surface carboxyl groups could be formed, whereas the reduction in nanotube length due to the chemical treatment was negligible. This chemical treatment was necessary to increase the interfacial adhesion between the PLA matrix and the nanotubes. In the direct blending of MWCNTs and polymers, carbon nanotubes tend to aggregate, and their nonuniform dispersion in the polymer matrix often results in deleterious effects. As shown in Figure 1(a) (TEM micrograph), the MWCNT–COOHs were homogeneously dispersed into the PLA ligaments, and no large aggregates were observed. Furthermore, with SEM and high magnification [Fig. 1(b)], we observed that the MWCNT–COOHs pulled out from the PLA matrix had a high adhesion with PLA because all of the nanotubes were covered with polymer. As already reported, because PLA has a lot of hydroxyl end groups, it is possible to create covalent or hydrogen bonds with the —COOH groups of MWCNTs.[22] In this study, the formation of hydrogen bonds between the polymer matrix and MWCNT–COOHs was proven by the Fourier transform infrared (FTIR) spectra. As shown in Figure 2(a), PLA had a peak at 3662 cm^{-1} for hydroxyl end groups and a peak at 3505 cm^{-1} for the carbonyl overtone. In the nanocomposites, the absorption band of the carbonyl

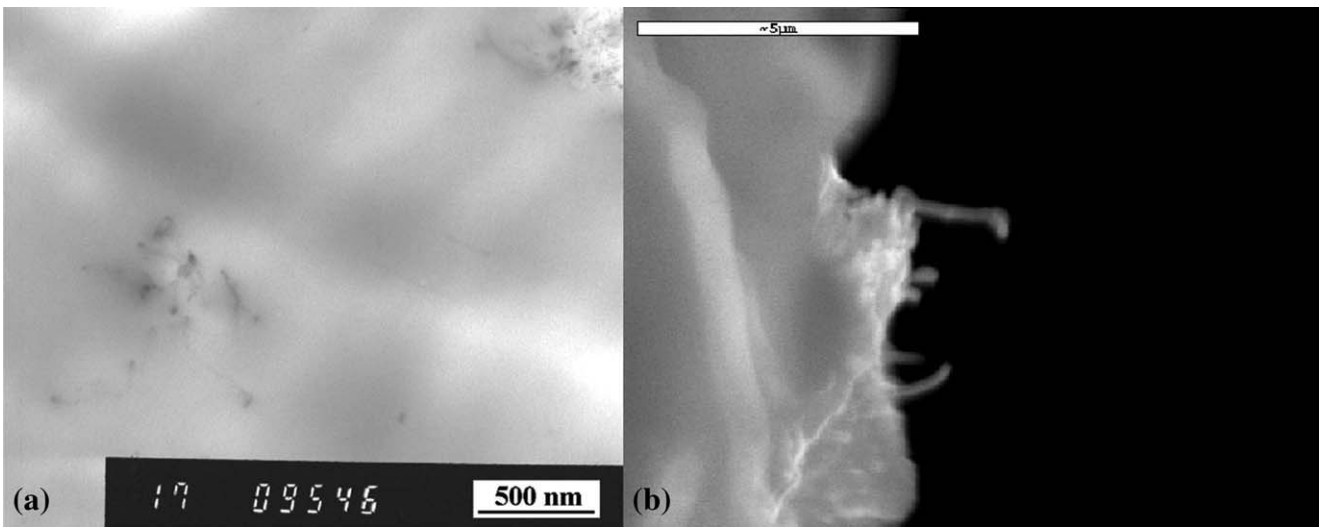

Figure 1 Micrographs of the PLA/MWCNT–COOH nanocomposites (2.5 wt % MWCNT–COOH): (a) TEM and (b) SEM micrographs.

group remained stable, whereas the corresponding absorption of the hydroxyl groups shifted to a lower wave number. Similar shifts were also recorded at the area 1000–1150 cm^{-1} [Fig. 2(b)] where the characteristic C—O bands of PLA were recorded. This hydrogen-bond formation and high adhesion between the PLA and MWCNT–COOHs enhanced the mechanical properties of the prepared nanocomposites.

From the stress–strain curves of the neat PLA and PLA/MWCNT–COOH nanocomposites with different MWCNT–COOH loadings, we found that the neat PLA was a very brittle material, as it exhibited yielding with a short quasi-constant stress regime, and failed at about 10% strain. The addition of the MWCNT–COOHs to PLA resulted in similar behavior with slight increase in elongation. In the PLA/MWCNT–COOH nanocomposites, the strain at break increased to about 20%, with negligible differences between the samples. This was in agreement with a previous study of Jiang et al.,[23] where it was found that the elongation at break of PLA increased with the incorporation of montmorillonite nanoparticles. Furthermore, a small increase was also recorded in the tensile strength at the yield point (σ_y) and σ_b. Neat PLA had a σ_y of about 63.5 MPa and a σ_b of about 58.2 MPa (Table I). The corresponding values increased in all of the studied nanocomposites with increasing MWCNT–COOH content, and the nanocomposite containing 2.5 wt % MWCNT–COOH broke at 85.5 and 73.6 MPa, respectively. The improved mechanical properties clearly showed the reinforcing action of the MWCNT–COOHs because, as the neat material had a high tensile strength, the

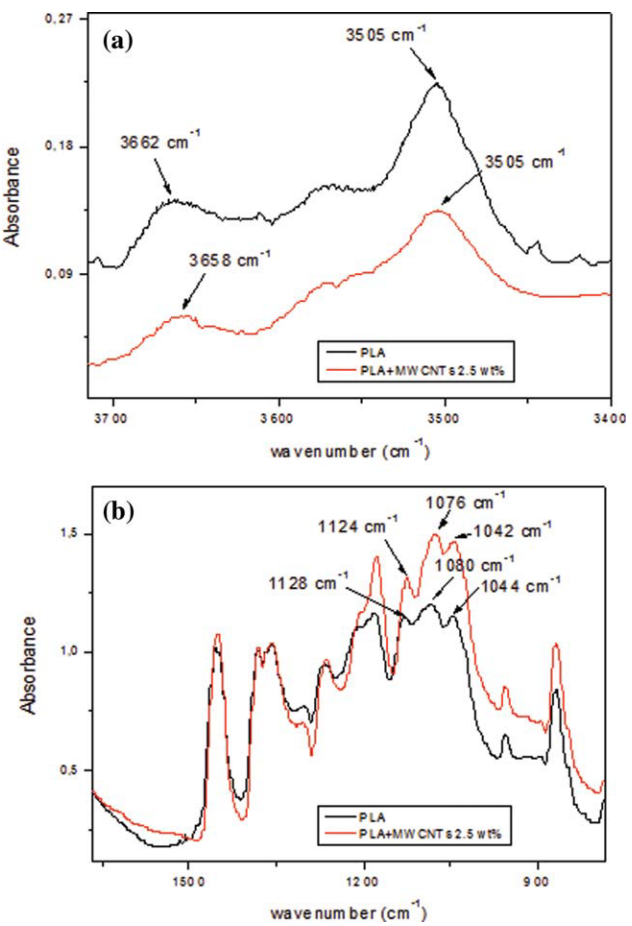

Figure 2 FTIR spectra of PLA and the PLA/MWCNT–COOH nanocomposites containing 2.5 wt % MWCNT–COOH at different wave-number areas. [Color figure can be viewed in the online issue, which is available at www.interscience.wiley.com.]

TABLE I
Mechanical Properties of the PLA/MWCNT–COOH Nanocomposites

Sample	σ_y (MPa)	σ_b (MPa)	Elongation at break (%)	Young's modulus (MPa)
PLA	63.5 ± 2.1	58.2 ± 1.5	10 ± 1	553 ± 25
PLA–MWCNT–COOH 0.5 wt %	65.4 ± 1.7	58.1 ± 1.9	19 ± 2	632 ± 32
PLA–MWCNT–COOH 1 wt %	70.2 ± 1.5	60.9 ± 1.7	20 ± 2	786 ± 41
PLA–MWCNT–COOH 2.5 wt %	85.5 ± 2.3	73.6 ± 2.2	19 ± 2	997 ± 26
PLA–MWCNT 2.5 wt %	59.5 ± 1.9	56.5 ± 2.1	10 ± 2	743 ± 32

nanotubes' incorporation into the PLA matrix resulted in the efficient transfer of mechanical load from the polymer matrix to the nanotubes.

Comparing the mechanical properties of the nanocomposite containing 2.5 wt % nonoxidized MWCNTs, we observed that both σ_y and σ_b were lower than those of neat PLA and, of course, much lower than those of the corresponding sample containing MWCNT–COOHs (Table I). This was additional evidence that the produced MWCNT–COOHs had higher adhesion with the PLA matrix than the untreated MWCNTs. This was due to the formed surface reactive groups, which as found from FTIR analysis, could create hydrogen bonds with the PLA reactive groups. Therefore, we concluded that the oxidation of the MWCNTs was an efficient way to produce nanocomposites with higher performance. The only benefit from the addition of nonoxidized MWCNTs was the calculated increase in Young's modulus.

Among the mechanical properties of the composites, of primary importance was σ_y. This parameter, which depends mainly on the microstructure, depends also on the interfacial bonding and on the form and size distribution of the filler, its spatial distribution in the matrix, the thickness of the interface, and so on. When there is poor bonding between the matrix and the filler, the composite will be brittle because the applied load cannot be transferred to the filler. On composite toughening, it is believed that when σ_b is lower than σ_y ($\sigma_b < \sigma_y$), a brittle fracture occurs. Yielding is the predominant deformation mechanism when the opposite occurs, that is, when $\sigma_b \geq \sigma_y$, and the fracture is ductile. So, as shown in Table I, although there was a substantial increase in σ_b after MWCNT–COOH incorporation, all of the studied nanocomposites could be characterized as brittle materials. In all of the nanocomposites, σ_y was higher than σ_b. Furthermore, Young's modulus of the studied nanocomposites significantly increased with MWCNT–COOH concentration. As shown in Table I, PLA had a value of 553 MPa, whereas in the case of the nanocomposites containing 2.5 wt % MWCNT–COOHs, the modulus was nearly doubled (997 MPa). This, in combination with the achieved increase in σ_b, verified that MWCNT–COOH incorporation enhanced the mechanical performance of the PLA ligaments, which was one of the main objectives of this study.

Thermal analysis

The melting point of PLA was recorded at 170.8°C, whereas in the nanocomposites, a slight increase was found when the amount of MWCNT–COOHs was increased. Thus, the sample containing 2.5 wt % MWCNT–COOH presented a melting point at 174.6°C [Fig. 3(a)]. This was attributed to a nucleation effect by the nanotubes, which increases the degree of crystallinity (X_c) of polyesters[24] and was in agreement with a previous study, where it was found that the equilibrium T_m obtained from Hoffman–Weeks plots increased with increasing nanotube content.[25] This was also confirmed from the values of the heat of fusion, which in all nanocomposites was higher than the corresponding values of neat PLA (Table II). Thus, X_c of the nanocomposites, as calculated on the basis of the enthalpy of fusion of 100% crystalline PLA, which was 93 J/g,[26] increased with increasing MWCNT–COOH content.

The nucleation effect of the MWCNT–COOHs on PLA crystallization was indicated more characteristically from T_{cc} measurements. The T_{cc} values of the nanocomposites were lower than that of neat PLA [Fig. 3(b)]. For example, T_{cc} decreased from 103°C for neat PLA to 101°C for PLA containing 1 wt % MWCNT–COOHs and to 99°C for PLA containing 2.5 wt % MWCNT–COOHs. The decrease in T_{cc} indicated that the cold crystallization of PLA in the nanocomposites became easier than in neat PLA. This lower T_{cc} was attributed to the MWCNT–COOHs, which acted as nucleating agents and enhanced the crystallization of the PLA macromolecules. This was probably due to the fact that the nanoparticles had a higher surface area in contact with semicrystalline polymer matrices and, thus, induced a heterogeneous nucleation effect.[24,27–30] A similar trend was also found in T_c from the melt. As shown in Table II, PLA crystallized at 100°C during cooling, whereas this temperature shifted to higher values with increasing MWCNT–COOH content.

Differences were also recorded in T_g of PLA after the addition of MWCNT–COOHs. Usually, the T_g of a polymeric matrix tends to increase with the

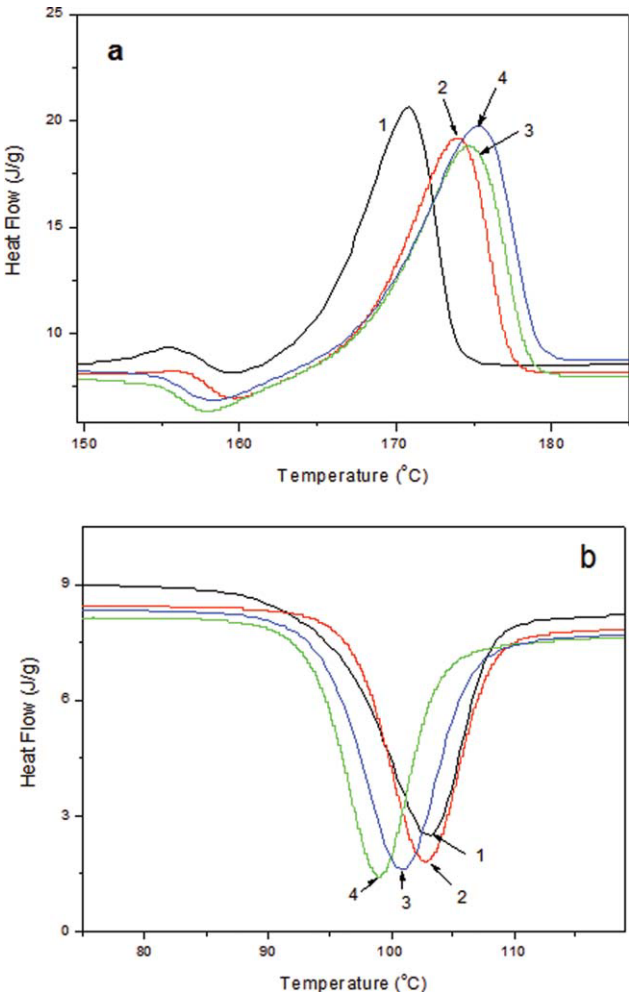

Figure 3 Thermal analysis of the PLA/MWCNT–COOH nanocomposites: (a) melting point and (b) T_{cc}. (1) PLA, (2) PLA–MWCNTs 0.5 wt %, (3) PLA–MWCNTs 1 wt %, and (4) PLA–MWCNTs 2.5 wt %. [Color figure can be viewed in the online issue, which is available at www.interscience.wiley.com.]

addition of nanoparticles because of the interactions between the polymer chains and the nanoparticles and because of the reduction of macromolecular chain mobility at the zone surrounding the nanoparticles.[31,32] The neat PLA was characterized by a T_g at 59.2°C. The addition of MWCNT–COOHs had a small effect on T_g, and as shown in Table II, the addition of 2.5 wt % MWCNT–COOHs to the neat PLA was followed by an increase in T_g of about 2°C. The glass transition is a complex phenomenon depending on a number of factors, including chain flexibility, molecular weight, branching, crosslinking, intermolecular interactions, and steric effects. The increase in T_g after the addition of the MWCNT–COOHs could have been due to the decrease in free volume in the polymer matrix due to the physical crosslinking caused by the interactions taking place between the carboxyl groups of the MWCNT–COOHs and PLA. As shown by FTIR spectroscopy, the surface of the MWCNT–COOHs had favorable interactions, such as hydrogen bonds, with the polymer chains. This should have contributed to the immobilization of the polymer chains that were adjacent to the MWCNT–COOHs and, thus, caused an increase in T_g. Thus, the small increase was attributed to the restriction of the mobility of the polymer chains as a consequence of bonding or adsorption on the MWCNT–COOH surface. A similar increase was also reported in PLA/MWCNT nanocomposites because of the existence of rigid MWCNTs incorporated into the PLA matrix[20] or in other nanocomposites, such as those with clay.[33]

DMA

DMA is a useful and very sensitive technique for investigating the microstructure of macromolecular chain conformations and movements during the exposure of polymers to a range of temperatures. In Figure 4(a) are presented the storage moduli as a function of temperature for neat PLA and its nanocomposites containing different amounts of MWCNT–COOHs. The storage modulus of neat PLA remained stable to 45°C and decreased at temperatures close to the glass transition. However, after this temperature area, the storage modulus increased slightly again with increasing temperature. This is unusual in polymers because the storage modulus decreases gradually with increasing temperature, and the recorded increase in the studied materials was attributed to the cold crystallization of PLA. Similar behavior was also observed in all of the nanocomposites. However, the most characteristic difference was that the storage modulus of the PLA/MWCNT–COOH nanocomposites tended to increase with increasing amount of MWCNT–

TABLE II
Thermal Properties of the PLA/MWCNT–COOH Nanocomposites

Sample	T_m (°C)	T_g (°C)	T_c (°C)	T_{cc} (°C)	ΔH_m (J/g)	X_c (%)
PLA	170.8	59.2	100.0	103.0	50.6	54.4
PLA–MWCNT 0.5 wt %	173.9	59.6	101.2	102.5	51.4	55.3
PLA–MWCNT 1 wt %	174.6	60.4	102.0	101.0	52.3	56.2
PLA–MWCNT 2.5 wt %	175.3	61.9	104.1	99.0	53.8	57.8

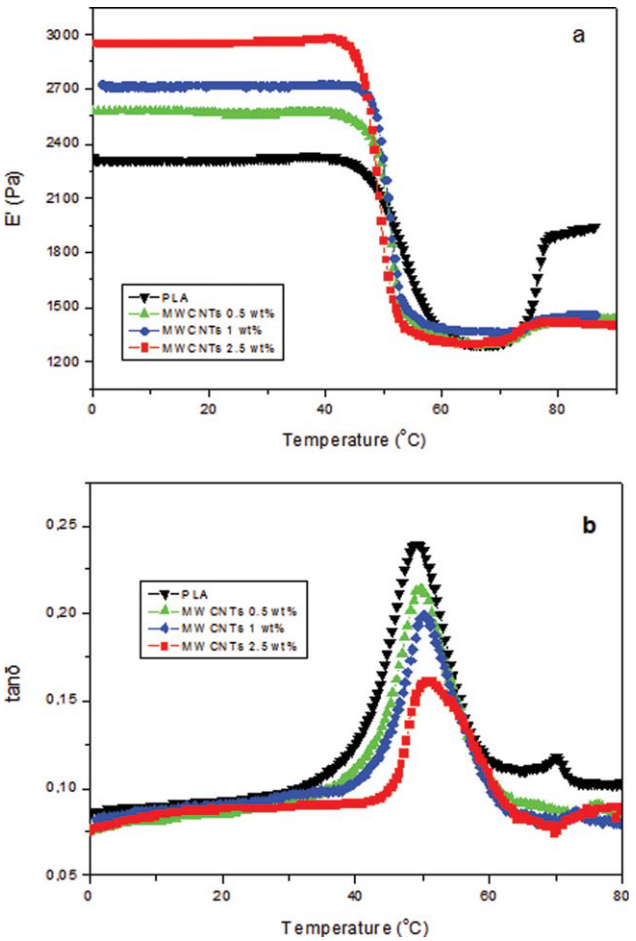

Figure 4 Dynamic mechanical relaxation behavior of the prepared PLA/MWCNT–COOH nanocomposites: (a) storage modulus (E') and (b) tan δ. [Color figure can be viewed in the online issue, which is available at www.interscience.wiley.com.]

COOHs. This indicated the effectiveness of the MWCNT–COOH reinforcing effect for the PLA ligaments, as was already verified from the mechanical properties.

Many alterations were also recorded in the tan δ curves. Neat PLA was found to have a T_g at about 49°C [Fig. 4(b)], whereas the temperature of the maximum peak shifted to higher values and there was a gradual decrease in the peak area with increasing MWCNT–COOH content. Thus, for the sample containing 2.5 wt % MWCNT–COOHs, T_g shifted up to 51.5°C.

This behavior was additional proof of the molecular movement restriction of PLA, which was due to the fine dispersion of MWCNT–COOHs, which led to greater interaction with the polymer matrix. Additionally, the reaction between the two phases and the formation of hydrogen bonds further limited the movement of polymer molecules. These findings were in good agreement with the results of DSC analysis.

Thermal stability

With regard to the thermal stability in general, the addition of a filler can improve the thermal stability of filled polymer composite systems to some extent, and the filler plays an important role. The TG and derivative thermogravimetric (DTG) curves of the PLA and PLA/MWCNTs nanocomposites with different concentrations of MWCNT–COOHs at a β of 10°C/min are shown in Figure 5(a,b). At about 261°C, PLA began to decompose and completed the decomposition at about 400°C; its maximum decomposition rate was at 361.3°C. The PLA/MWCNT–COOH nanocomposites began to decompose at a higher temperature (∼ 287°C) and completed the decomposition at about the same temperature as PLA. According to Wu et al.,[16] the addition of carbon nanotubes increases the onset of the decomposition temperature by about 10–20°C or even more. This is an indication that the addition of MWCNT–COOHs causes a substantial thermal enhancement

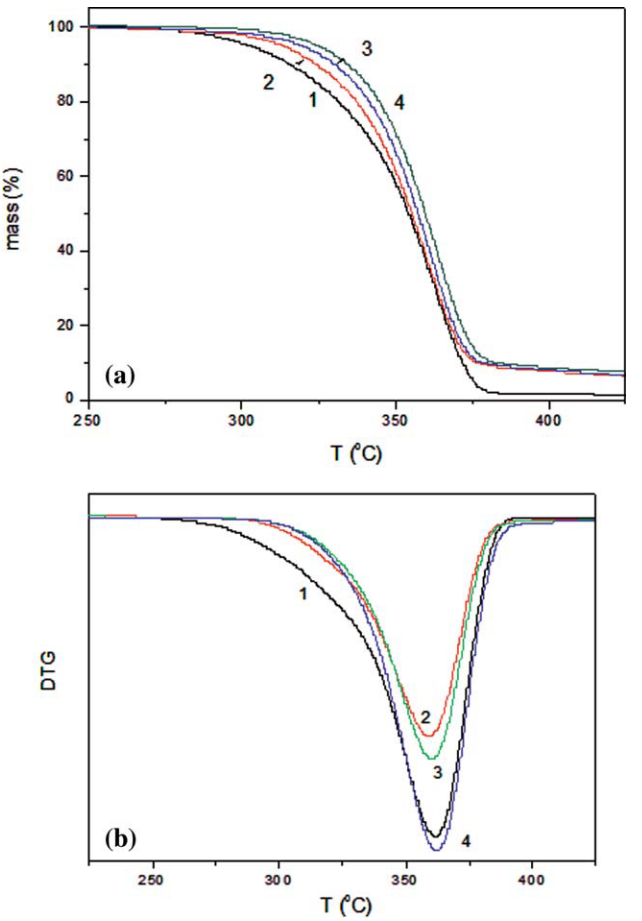

Figure 5 (a) TG and (b) DTG curves of the PLA/MWCNT nanocomposites for β = 10°C/min: (1) PLA, (2) PLA–0.5% MWCNTs, (3) PLA–1% MWCNTs, and (4) PLA–2.5% MWCNTs. [Color figure can be viewed in the online issue, which is available at www.interscience.wiley.com.]

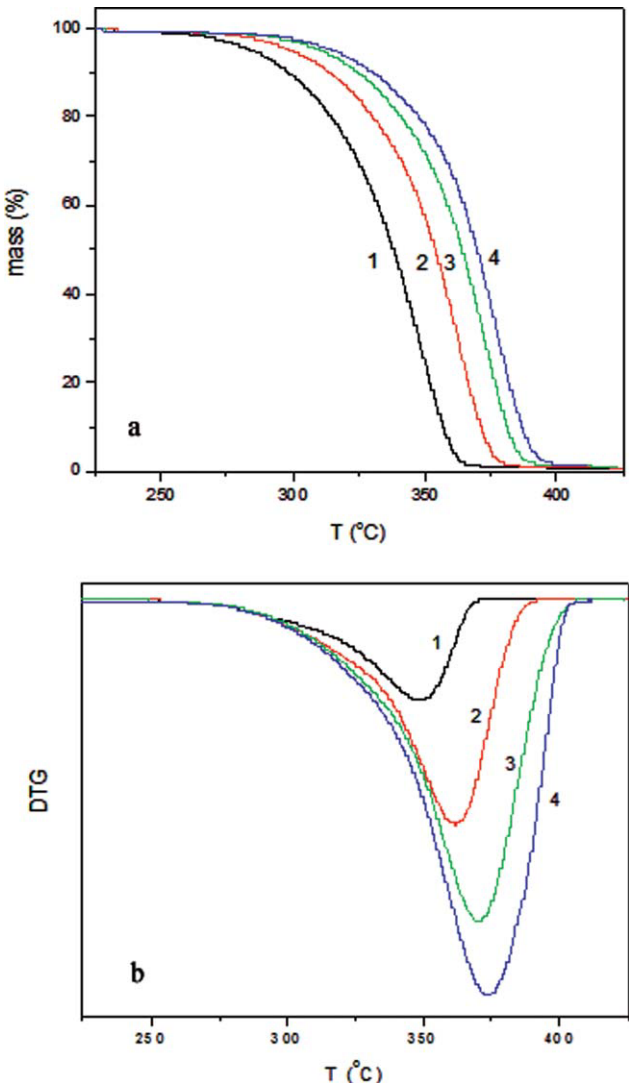

Figure 6 (a) TG and (b) DTG curves of PLA at different β's: (1) 5, (2) 10, (3) 15, and (4) 20°C/min. [Color figure can be viewed in the online issue, which is available at www.interscience.wiley.com.]

of PLA, at least in the initial stages of decomposition. This improvement is mainly attributed to good matrix–nanotube interactions, good thermal conductivity of the nanotubes, and their barrier effect. However, although the nanocomposites began to decompose at higher temperatures, the addition of MWCNT–COOHs seemed to have little effect on the temperature at which the maximum decomposition rate took place.

Determination of *E*

From the three different concentrations of MWCNT–COOH, we chose to analyze the samples with the higher concentration of MWCNT–COOHs compared to that of PLA. The TG and DTG curves of PLA and PLA with 2.5 wt % MWCNT–COOHs at different β's (5, 10, 15, and 20°C/min) are shown in Figures 6 and 7. The TG curves shifted to higher temperatures as β increased from 5 to 20°C/min. The shift of onset to higher temperatures with increasing β was due to the shorter time required for the sample to reach a given temperature at faster β's. This β dependence was also indicated by the DTG curves, with the DTG peaks shifting toward higher temperatures with increasing β.

For the determination of *E*, we choose to use and compare two different methods, the Ozawa–Flynn–Wall (OFW) and Friedman methods, because every method has its own error. First, the isoconversional OFW method was used to calculate the *E* values of PLA and PLA/MWCNT–COOH 2.5 wt % for different conversion values with the following equation:

$$\ln \beta = -1.0516 \frac{E}{RT} + \text{Constant}$$

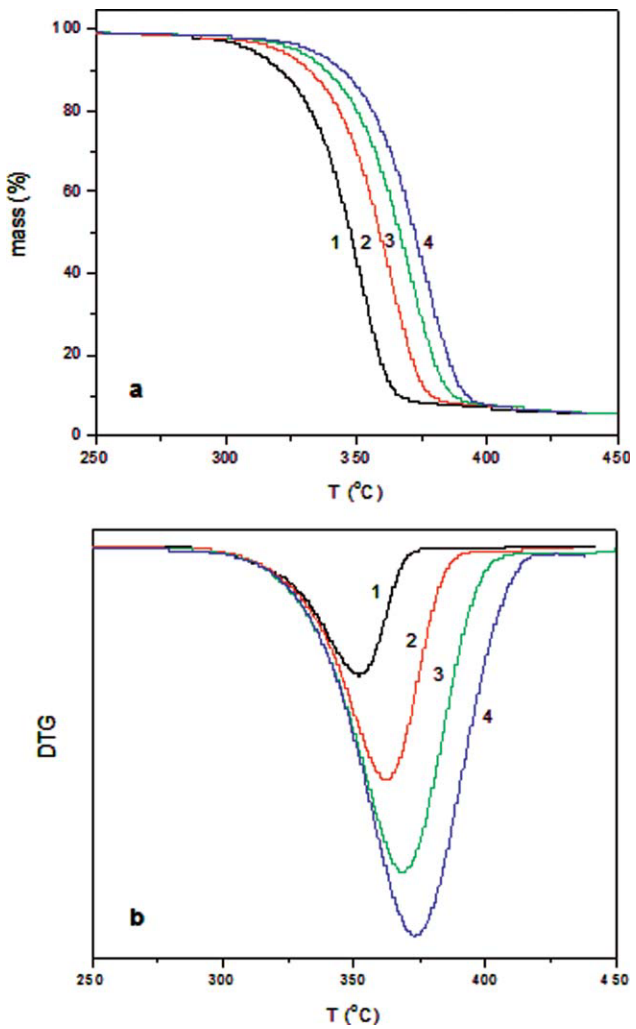

Figure 7 (a) TG and (b) DTG curves of the PLA–MWCNT–COOH 2.5 wt % nanocomposites at different β's: (1) 5, (2) 10, (3) 15, and (4) 20°C/min. [Color figure can be viewed in the online issue, which is available at www.interscience.wiley.com.]

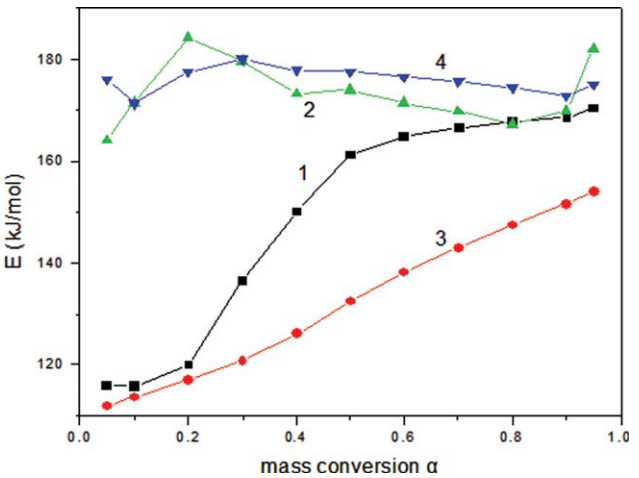

Figure 8 *E* as calculated with the OFW and Friedman methods versus α: (1) Friedman, PLA; (2) Friedman, PLA–2.5 wt % MWCNT–COOH; (3) OFW, PLA; and (4) OFW, PLA–2.5 wt % MWCNT–COOH. [Color figure can be viewed in the online issue, which is available at www.interscience.wiley.com.]

where T is the temperature and R is the gas constant. Second, the Friedman method was used, and E was calculated with the following equation:

$$\ln\left(\beta\frac{d\alpha}{dT}\right) = \ln A + \ln f(\alpha) - \frac{E}{RT}$$

where α is the degree of conversion, $f(\alpha)$ is the conversion function (reaction model), and A is the preexponential factor. The calculated values of E for different values of α are shown in Figure 8. The difference in the E values calculated by the two methods could be explained by a systematic error due to improper integration. The method of Friedman employs instantaneous rate values and, therefore, is very sensitive to experimental noise. In the Ozawa method, the equation used was derived with the assumption of a constant E; thus, a systematic error is introduced in the estimation of E in the case that E varies with α. This error can be estimated by comparison with the Friedman results.[34] As shown in Figure 8, for PLA, the dependence of E on α, as calculated with Friedman's method, could be separated into three distinct regions: the first for values of α up to 0.2, in which E was almost stable; the second, ($0.2 < \alpha < 0.5$) in which E presents a monotonous increase; and the third ($0.5 < \alpha < 0.95$), in which E could be considered as having a constant average value as in the first region. The different regions were not discriminated in the dependence of E from α as calculated with the OFW method because they presented a monotonous increase. This dependence of E on α was an indication of a complex reaction with the participation of at least two different mechanisms. As shown in Figure 8, for PLA/MWCNT–COOH containing 2.5 wt % MWCNT–COOHs, the dependence of E from α was not as complicated as it was for PLA. It showed only one region with a relatively constant value of E. Furthermore, when the E values of PLA and its nanocomposite were compared, it was clear that for all conversions, PLA had lower values than the nanocomposites. The differences were even higher at lower conversions, which corresponded to the initial decomposition stages. From the E values, it was clear that MWCNT–COOH had a thermal stabilizing effect on PLA decomposition.

The calculated values of E for PLA were in the area of the values presented in the literature, and the values of E for PLA/MWCNT–COOH 2.5 wt % were greater than those of Kim et al.,[17] showing the same trend in comparison with the value of E of PLA.

Effect of the MWCNT–COOHs on the PLA enzymatic hydrolysis

The addition of the MWCNT–COOHs into the PLA matrix had not only positive effects but may have also had some negative effects, as in the case of enzymatic hydrolysis. In Figure 9 are presented the plots of the percentage weight loss during enzymatic hydrolysis for several days of PLA and its nanocomposites containing different amounts of MWCNT–COOHs. In general, low hydrolysis rates were observed. This was because PLA and their nanocomposites had very high X_c values. However, neat PLA presented a higher weight loss compared with its nanocomposites. The differences in the hydrolysis rates were more obvious after the 3rd day of treatment. Additives, it is well known, can affect the hydrolytic degradation rates of aliphatic polyesters.

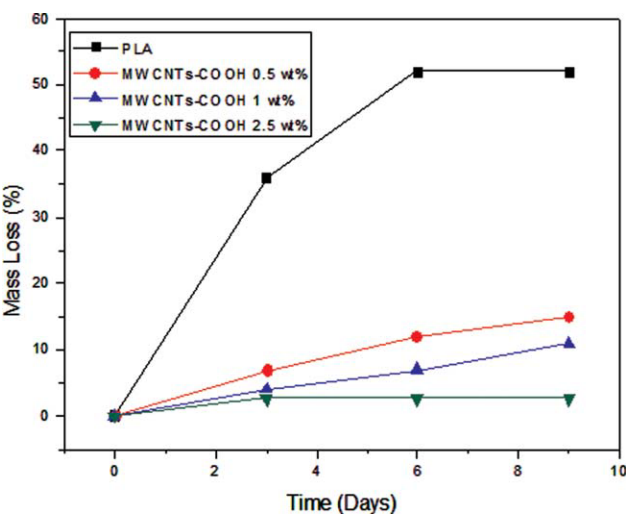

Figure 9 Weight loss as a function of the time of enzymatic hydrolysis for PLA and the PLA–MWCNT–COOH nanocomposites. [Color figure can be viewed in the online issue, which is available at www.interscience.wiley.com.]

Zhou and Xanthos[35] recently reported that the degradation rates were higher for amorphous PLA and its composites containing montmorillonite than for semicrystalline PLA and its composites with the same additive as a result of increased permeation through the amorphous domains. Furthermore, Chouzouri and Xanthos[36] found that the addition of calcium silicate and Bioglass 45S5 fillers appeared to enhance the degradation behavior of aliphatic polyesters, such as polycaprolactone and PLA.

These hydrophilic fillers appeared to increase the water uptake and the hydrophilicity of the polymer, and thus, the degradation rates due to enzymatic hydrolysis were higher. In a recent study,[37] it was reported that MWCNTs can also increase the hydrolysis rate of PLA. However, in the studied nanocomposites, the opposite trend was observed, and MWCNT–COOHs retarded the enzymatic hydrolysis of PLA. This may have been because X_c, as was verified from the DSC studies, was in all of the nanocomposites higher than in neat PLA or because the addition of the MWCNT–COOHs lowered the available surface of PLA for enzymatic hydrolysis.

CONCLUSIONS

The oxidative treatment of MWCNTs resulted in an increased adhesion with the PLA matrix and drastically affected the mechanical properties of the PLA/MWCNT–COOH nanocomposites. Remarkable increases were found in the tensile strength and Young's modulus of the nanocomposites; these also varied with the MWCNT–COOH amount. This is very important for PLAs that are used as reinforcement ligaments. The addition of untreated MWCNTs resulted in a slight deterioration in the mechanical properties.

The MWCNT–COOHs also acted as nucleating agents and increased X_c of PLA and its crystallization rate. The MWCNT–COOHs caused a heterogeneous nucleating effect because of their large available surface area.

All of the MWCNT–COOH nanocomposites showed higher thermal stabilities than neat PLA, but the lower the enzymatic hydrolysis rate of PLA may have been due to the higher X_c that the nanocomposites had or because the nanotubes lowered the available surface for hydrolysis.

References

1. Mooney, D. J.; Sano, K.; Kaufmann, M. P.; Majahod, K.; Schloo, B.; Vacanti, J. P.; Langer, R. J Biomed Mater Res 1997, 37, 413.
2. Proikakis, C. S.; Mamouzelos, N. J.; Tarantili, P. A.; Andreopoulos, A. G. Polym Degrad Stab 2006, 91, 614.
3. Chang, J. H.; An, Y. U.; Cho, D.; Giannelis, E. P. Polymer 2003, 44, 3715.
4. Bastioli, C. In Wiley Encyclopedia of Packaging Technology, 2nd ed.; Brody, A. L.; Marsh, K. S., Eds.; Wiley: New York, 1997; p 77.
5. Satyanarayana, D.; Chatterji, P. R. J Macromol Sci Rev Macromol Chem Phys 1993, 33, 349.
6. Griffith, G. L. Polym Biomater Acta Mater 2000, 48, 263.
7. Cheung, H. Y.; Lau, K. T.; Lu, T. P.; Hui, D. Compos B 2007, 38, 291.
8. Hutmacher, D. W. Biomaterials 2000, 21, 2529.
9. Molina, I.; Li, S.; Martinez, M. B.; Vert, M. Biomaterials 2001, 22, 363.
10. Chiang, M.-F.; Wu, T.-M. Compos Sci Technol 2010, 70, 110.
11. Wen, X.; Lin, Y.; Han, C.; Zhang, K.; Ran, X.; Li, Y.; Dong, L. J Appl Polym Sci 2009, 114, 3379.
12. Ozkoc, G.; Kemaloglu, S. J Appl Polym Sci 2009, 114, 2481.
13. Sangwan, P.; Way, C.; Wu, D.-Y. Macromol Biosci 2009, 9, 677.
14. Villmow, T.; Pötschke, P.; Pegel, S.; Häussler, L.; Kretzschmar, B. Polymer 2008, 49, 3500.
15. Wu, C.-S.; Liao, H.-T. Polymer 2007, 48, 4449.
16. Wu, D.; Wu, L.; Zhang, M.; Zhao, Y. Polym Degrad Stab 2008, 93, 1577.
17. Kim, H.; Park, B.; Yoon, J.; Jin, H. Eur Polym J 2007, 43, 1729.
18. Bikiaris, D.; Vassiliou, A.; Chrissafis, K.; Paraskevopoulos, K. M.; Jannakoudakis, A.; Docoslis, A. Polym Degrad Stab 2008, 93, 952.
19. Song, W.; Zheng, Z.; Tang, W.; Wang, X. Polymer 2007, 48, 3658.
20. Yoon, J. T.; Jeong, Y. G.; Lee, S. C.; Min, B. G. Polym Adv Technol 2009, 20, 631.
21. Kuan, C.-F.; Chen, C.-H.; Kuan, H.-C.; Lin, K.-C.; Chiang, C.-L.; Peng, H.-C. J Phys Chem Solids 2008, 69, 1399.
22. Kuan, C.-F.; Kuan, H.-C.; Ma, C.-C. M.; Chen, C.-H. J Phys Chem Solids 2008, 69, 1395.
23. Jiang, L.; Zhang, J.; Wolcott, M. P. Polymer 2007, 48, 7632.
24. Tzavalas, S.; Drakonakis, V.; Mouzakis, D. E.; Fisher, D.; Gregoriou, V. G. Macromolecules 2006, 39, 9150.
25. Shieh, Y.-T.; Liu, G.-L.; Twu, Y.-K.; Wang, T.-L.; Yang, C.-H. J Polym Sci Part B: Polym Phys 2010, 48, 145.
26. Migliaresi, C. D.; Cohn, D.; De Lollis, A.; Fambri, L. J Appl Polym Sci 1991, 43, 83.
27. Gopakumar, T. G.; Lee, J. A.; Kontopoulou. M.; Parent, J. S. Polymer 2002, 43, 5483.
28. Antoniadis, G.; Paraskevopoulos, K. M.; Bikiaris, D.; Chrissafis, K. Thermochim Acta 2009, 493, 68.
29. Antoniadis, G.; Paraskevopoulos, K. M.; Bikiaris, D.; Chrissafis, K. J Polym Sci Part B: Polym Phys 2009, 47, 1452.
30. Bailly, M.; Kontopoulou, M. Polymer 2009, 50, 2472.
31. Chrissafis, K.; Paraskevopoulos, K. M.; Papageorgiou, G. Z.; Bikiaris, D. N. J Appl Polym Sci 2008, 110, 1739.
32. Chen, K.; Wilkie, C. A.; Vyazovkin, S. J Phys Chem B 2007, 111, 12685.
33. Krishnamachari, P.; Zhang, J.; Lou, J.; Yan, J.; Uitenham, L. Int J Polym Anal Charact 2009, 14, 336.
34. Vyazovkin, S. J Comput Chem 2001, 22, 178.
35. Zhou, Q.; Xanthos, M. Polym Degrad Stab 2008, 93, 1450.
36. Chouzouri, G.; Xanthos, M. J Plastic Film Sheeting 2007, 23, 19.
37. Feng, J.; Sui, J.; Chakoli, A. N.; Cai, W. Int J Mod Phys B 2009, 23, 1503.